

See discussions, stats, and author profiles for this publication at: <https://www.researchgate.net/publication/12160703>

# A Differential Scanning Calorimetric and $^{31}\text{P}$ NMR Spectroscopic Study of the Effect of Transmembrane $\alpha$ -Helical Peptides on the Lamellar–Reversed Hexagonal Phase Transition of Phosp...

ARTICLE *in* BIOCHEMISTRY · FEBRUARY 2001

Impact Factor: 3.02 · DOI: 10.1021/bi001942j · Source: PubMed

---

CITATIONS

40

---

READS

16

4 AUTHORS, INCLUDING:



Robert S. Hodges

University of Colorado

494 PUBLICATIONS 21,647 CITATIONS

SEE PROFILE

# A Differential Scanning Calorimetric and $^{31}\text{P}$ NMR Spectroscopic Study of the Effect of Transmembrane $\alpha$ -Helical Peptides on the Lamellar–Reversed Hexagonal Phase Transition of Phosphatidylethanolamine Model Membranes<sup>†</sup>

Feng Liu, Ruthven N. A. H. Lewis, Robert S. Hodges, and Ronald N. McElhaney\*

Department of Biochemistry, University of Alberta, Edmonton, Alberta, Canada T6G 2H7

Received August 16, 2000; Revised Manuscript Received October 27, 2000

**ABSTRACT:** We have investigated the effects of the model  $\alpha$ -helical transmembrane peptide Ac-K<sub>2</sub>L<sub>24</sub>K<sub>2</sub>-amide (L<sub>24</sub>) on the thermotropic phase behavior of aqueous dispersions of 1,2-dielaidoylphosphatidylethanolamine (DEPE) to understand better the interactions between lipid bilayers and the membrane-spanning segments of integral membrane proteins. We studied in particular the effect of L<sub>24</sub> and three derivatives thereof on the liquid-crystalline lamellar (L <sub>$\alpha$</sub> )–reversed hexagonal (H<sub>II</sub>) phase transition of DEPE model membranes by differential scanning calorimetry and  $^{31}\text{P}$  nuclear magnetic resonance spectroscopy. We found that the incorporation of L<sub>24</sub> progressively decreases the temperature, enthalpy, and cooperativity of the L <sub>$\alpha$</sub> –H<sub>II</sub> phase transition, as well as induces the formation of an inverted cubic phase, indicating that this transmembrane peptide promotes the formation of inverted nonlamellar phases, despite the fact that the hydrophobic length of this peptide exceeds the hydrophobic thickness of the host lipid bilayer. These characteristic effects are not altered by truncation of the side chains of the terminal lysine residues or by replacing each of the leucine residues at the end of the polyleucine core of L<sub>24</sub> with a tryptophan residue. Thus, the characteristic effects of these transmembrane peptides on DEPE thermotropic phase behavior are independent of their detailed chemical structure. Importantly, significantly shortening the polyleucine core of L<sub>24</sub> results in a smaller decrease in the L <sub>$\alpha$</sub> –H<sub>II</sub> phase transition temperature of the DEPE matrix into which it is incorporated, and reducing the thickness of the host phosphatidylethanolamine bilayer results in a larger reduction in the L <sub>$\alpha$</sub> –H<sub>II</sub> phase transition temperature. These results are not those predicted by hydrophobic mismatch considerations or reported in previous studies of other transmembrane  $\alpha$ -helical peptides containing a core of an alternating sequence of leucine and alanine residues. We thus conclude that the hydrophobicity and conformational flexibility of transmembrane peptides can affect their propensity to induce the formation of inverted nonlamellar phases by mechanisms not primarily dependent on lipid–peptide hydrophobic mismatch.

The complex mixture of lipids present in prokaryotic and eukaryotic cell membranes typically forms only a liquid-crystalline lamellar (L <sub>$\alpha$</sub> )<sup>1</sup> phase under physiologically relevant conditions (1–2). However, the individual lipid classes present in such membranes can form either lamellar or nonlamellar phases when dispersed in excess water (3–5). In prokaryotic cell membranes, the uncharged diglycosyl diacylglycerol and anionic phosphatidylglycerol and cardiolipin components prefer the lamellar phase, their uncharged

monoglycosyl diacylglycerol and zwitterionic PE components prefer inverted hexagonal and cubic phases, and certain anionic phosphorylated glycolipid components prefer the normal micellar phase (6, 7). Similarly, in eukaryotic membranes, the zwitterionic PC and sphingomyelin components and the anionic phosphatidylserine component prefer the lamellar phase, the zwitterionic phospholipid component PE prefers the H<sub>II</sub> phase, while the anionic, complex glycosphingolipid (ganglioside) components prefer the normal micellar phase at neutral pH and physiological ionic strength. A considerable body of evidence has now accumulated indicating that these nonlamellar phase-preferring lipid components, as well as the various lamellar phase-preferring lipid components, play important structural and functional roles in eukaryotic membranes (for a review, see ref 8).

The phase that a fully hydrated membrane lipid prefers under a given set of conditions can be rationalized by considering the geometric packing of lipid molecules in various aggregates, which can in turn be described by a packing parameter or shape factor characteristic of the lipid molecule under these conditions (see refs 9 and 10). For a

<sup>†</sup> This work was supported by operating and major equipment grants from the Canadian Institutes of Health Research and by major equipment grants from the Alberta Heritage Foundation for Medical Research. F.L. was supported in part by a 75<sup>th</sup> Anniversary Studentship award by the Faculty of Medicine, University of Alberta.

\* Corresponding author. Phone: (780) 492-2413. Fax: (780) 492-0095. E-mail: rmcclhan@gpu.srv.ualberta.ca.

<sup>1</sup> Abbreviations: DSC, differential scanning calorimetry; NMR, nuclear magnetic resonance; PE, phosphatidylethanolamine; DEPE, dielaidoylphosphatidylethanolamine; DPEPE, dipalmitelaidoylphosphatidylethanolamine; L <sub>$\alpha$</sub> , lamellar liquid-crystalline; L <sub>$\beta$</sub> , lamellar gel; H<sub>II</sub>, inverted (or reversed) hexagonal; T<sub>h</sub>, liquid-crystalline lamellar–inverted hexagonal transition temperature; L<sub>24</sub>, Ac-K<sub>2</sub>-L<sub>24</sub>-K<sub>2</sub>-amide; P<sub>24</sub>, Ac-G-K<sub>2</sub>-L<sub>24</sub>-K<sub>2</sub>-A-amide; W-L<sub>22</sub>-W, Ac-K<sub>2</sub>-W-L<sub>22</sub>-W-K<sub>2</sub>-amide; L<sub>24</sub>-DAP, Ac-(DAP)<sub>2</sub>-L<sub>24</sub>-(DAP)<sub>2</sub>-amide; P<sub>16</sub>, Ac-K<sub>2</sub>-G-L<sub>16</sub>-K<sub>2</sub>-A-amide; DAP, L-2,3-diaminopropionic acid.

series of different phospholipids having the same number and type of hydrocarbon chains, this parameter is in turn determined primarily by the optimal area occupied by the polar headgroup at the lipid–water interface. If the conformations of the various phospholipid polar headgroups are generally similar, the optimal area occupied by the polar headgroups should be approximately proportional to headgroup size (7, 11–13). However, second-order but nevertheless potentially important interactions can also affect the optimal headgroup area and thus the effective shape of the lipid molecule, including attractive hydrogen-bonding and electrostatic interactions with adjacent polar headgroups. With liquid-crystalline PE bilayers, the combination of the relatively small size of the polar headgroups and their capacity for electrostatic and hydrogen-bonding attraction to adjacent polar headgroups results in significant negative curvature stress, which is the driving force behind their propensity to form H $_2$  phases at higher temperatures. The modulation of both lipid packing and curvature stress by inclusions, such as proteins and peptides, can markedly affect the lamellar/nonlamellar phase behavior of lipid membranes (for reviews, see refs 13 and 14).

The synthetic peptide P $_{24}$  and its analogues have been successfully used as a model of the hydrophobic transmembrane  $\alpha$ -helical segments of the integral membrane proteins (15, 16). These peptides are composed of a long sequence of hydrophobic leucine residues capped at both the N- and C-termini by two positively charged, relatively polar lysine residues. The poly-leucine core of these peptides forms a hydrophobic  $\alpha$ -helix that is intended to span the lipid bilayer, while the somewhat polar positively charged lysine residues at the N- and C-termini serve to anchor these termini to the bilayer surface and to inhibit lateral aggregation. The  $\alpha$ -helical conformation and transbilayer orientation of these peptides within lipid bilayers have been proven by a combination of CD (4), FTIR (17–19), X-ray diffraction (20), and fluorescence quenching (21) measurements. DSC (15, 17) and  $^2\text{H}$  NMR spectroscopic (15, 22, 23) studies also indicate that the incorporation of these peptides into PC and PE bilayers broadens the gel–liquid-crystalline phase transition and reduces its enthalpy. It has also been demonstrated that the effects of these peptides on PC bilayers are dependent on both the sign and magnitude of the mismatch between peptide hydrophobic length and membrane hydrophobic thickness (17). However, comparable hydrophobic mismatch effects are not observed when P $_{24}$  is incorporated into PE bilayers (24). In addition,  $^2\text{H}$  NMR spectroscopic studies (25) have shown that in the rotational motion of P $_{24}$  about its long axis perpendicular to the membrane plane is severely restricted in the gel state but quite rapid in the liquid-crystalline state. Finally, ESR (26) results show that a closely related peptide, L $_{24}$ , exists at least primarily as a monomer in liquid-crystalline PC bilayers, even at relatively high peptide concentrations.

In this study, the synthetic phospholipid DEPE was used as the primary matrix lipid to study transmembrane peptide–lipid interactions generally and the effect of these peptides on the L $\alpha$ –H $_2$  phase equilibrium in particular. This lipid is well-suited for these studies because its L $\beta$ –L $\alpha$  and L $\alpha$ –H $_2$  phase transition temperatures occur at experimentally convenient temperatures [ $\sim 37$  and  $\sim 65$  °C, respectively (3)] and because its hydrocarbon chain length closely matches

that of the most common lipid species present in most eukaryotic and prokaryotic membranes (1). Many previous studies have shown that DEPE is an excellent matrix for investigating the relative effects of lipophilic additives on lipid lamellar/nonlamellar phase behavior (see ref 12 and references therein). Other studies have shown that naturally occurring peptides such as alamethicin, gramicidin A, and gramicidin S all promote nonlamellar phase formation when incorporated into DEPE dispersions (27–30). Moreover, recent experiments with the WALP peptides have shown that synthetic  $\alpha$ -helical transmembrane peptides may have a profound effect on the lamellar/nonlamellar phase behavior of DEPE, depending on the mismatch between the hydrophobic length of the peptide and the hydrophobic thickness of DEPE bilayers (31).

In this study, we investigate the effects of the  $\alpha$ -helical transmembrane peptide L $_{24}$  and other structurally related peptides on the L $\alpha$ –H $_2$  phase equilibrium of a DEPE matrix. The examined structural derivatives were used to evaluate several hypotheses related to the effects of peptide–lipid hydrophobic mismatch on the lamellar/nonlamellar phase behavior of phospholipid model membranes. First, with the peptide L $_{24}$ -DAP, the two pairs of capping lysine residues at the end of L $_{24}$  have been replaced with the lysine analogues DAP, in which three of the four side chain methylene groups have been removed. This peptide was used to test the so-called snorkel model first suggested by Segrest et al. (32) to explain the behavior of positively charged residues in the amphipathic helices present at the surfaces of blood lipoproteins and later extended to transmembrane  $\alpha$ -helices by von Heijne et al. (33). According to the transmembrane peptide version of the snorkel model, the long, flexible hydrophobic side chains of lysine or arginine can extend along the transmembrane helix so that the terminal charged moiety can reside in the lipid polar headgroup region while the  $\alpha$ -carbon of the amino acid residue remains well below (or possibly above) the membrane–water interface, even when the hydrophobic length of the peptide is considerably different from that of the host lipid bilayer. Because of the shorter spacer arms between the charged group and the  $\alpha$ -carbon of DAP, the peptide L $_{24}$ -DAP is expected to be less accommodating to hydrophobic mismatch and any effects of such mismatch on the thermotropic phase behavior of its host lipid bilayer should be exaggerated.

Second, to investigate the importance of interfacially located tryptophan residues with respect to the effects of transmembrane peptides on their host lipid bilayer, we have examined the effect of the peptide W-L $_{22}$ -W on the lamellar/nonlamellar phase behavior of DEPE membranes. W-L $_{22}$ -W is an L $_{24}$  derivative in which the residues Leu-3 and Leu-26 are replaced with tryptophans. The preference of tryptophan and tyrosine residues for membrane polar–apolar interfaces is found to be one of the common features of natural membrane proteins (34). Previous studies have shown that interfacially localized tryptophan residues are necessary for the promotion of H $_2$  phases by the peptide gramicidin A and that N-formylation of these tryptophan residues completely and reversibly blocks the capacity of gramicidin A to induce H $_2$  phase formation in dioleoylphosphatidylcholine model membranes (35–37). In addition, recent studies of the WALP model transmembrane peptides (for details on the structures of these peptides, see refs 39 and 45) have

shown that these peptides can promote the formation of inverted nonlamellar phases in PC and PE model membranes and that interfacially localized tryptophans markedly enhance their capacity to do so (32, 38–40).

Finally, to address more directly the issue of peptide hydrophobic mismatch on membrane lamellar/nonlamellar phase behavior, we have studied the effect of the P<sub>16</sub> peptide on the lamellar/nonlamellar phase equilibrium of DEPE and have also examined the effect of the longer peptides such as L<sub>24</sub> on the lamellar/nonlamellar phase behavior of DPEPE. The P<sub>16</sub> peptide is a structural analogue of P<sub>24</sub>, with a shorter hydrophobic polyleucine core (16 rather than 24 leucine residues), and DPEPE is a shorter chain homologue of DEPE which forms bilayers with a reduced hydrophobic thickness. In contrast to previous findings with the WALP and KALP transmembrane peptides, we find no evidence for hydrophobic mismatch effects playing the major role in determining the effects of L<sub>24</sub> and related peptides on the L<sub>α</sub>–H<sub>II</sub> phase equilibrium of the host PE matrix.

## MATERIALS AND METHODS

The peptides P<sub>16</sub>, L<sub>24</sub>, L<sub>24</sub>-DAP, and W-L<sub>22</sub>-W were synthesized and purified using the solid phase synthetic methodology and the high-performance liquid chromatographic procedures described by Zhang et al. (41). Phospholipids were obtained from Avanti Polar Lipids Inc. (Birmingham, AL) and used without further purification. Lipid/peptide vesicle suspensions were prepared as follows. The lipid and peptide were codissolved in methanol in a clean glass test tube in proportions appropriate for the required lipid:peptide ratio. The solution was concentrated with a stream of nitrogen to a small volume (~0.1 mL), and approximately 4 mL of benzene was added. The sample was then frozen with dry ice and acetone and lyophilized in vacuo overnight. The powdery sample that was obtained was hydrated by vigorous vortexing in a buffer [50 mM Tris and 100 mM NaCl (pH 7.4)] at temperatures near 50 °C. For the DSC experiments, 0.5 mL samples containing 2 mg of lipid were analyzed with a Microcal-VP-DSC high-sensitivity microcalorimeter (Microcal Software Inc., Northampton, MA) operating at scan rates near 30 °C/h except where noted. Data were normally acquired during three cycles of heating and cooling scans and were analyzed with the Origin software package (Microcal Software Inc.). The reported transition midpoints represent the temperatures at which 50% conversion occurs based on the areas of the DSC peaks. All of the DSC experiments reported here were carried out twice, and the results of each set of experiments were very similar. For the <sup>31</sup>P NMR spectroscopic experiments, samples typically containing 10 mg of lipid were dispersed in the same buffer used for the DSC experiments by three cycles of vigorous vortexing at temperatures near 50 °C and cooling to 0 °C. Samples were then cooled to temperatures near 0 °C prior to initial data acquisition in the heating mode. <sup>31</sup>P NMR spectra were recorded with a Varian Unity 300 spectrometer (Varian Instruments, Palo Alto, CA) operating at 121.42 MHz for <sup>31</sup>P. Data were recorded and processed using the data acquisition and data processing parameters described by Lewis et al. (42) and were plotted with the Origin software package.

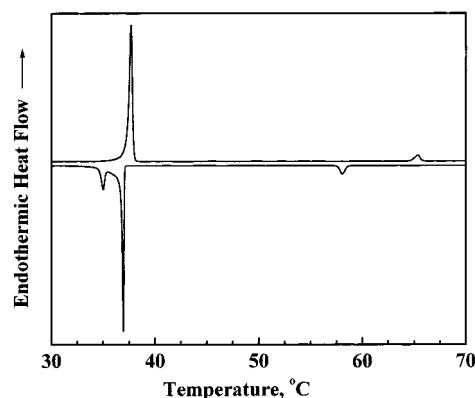


FIGURE 1: DSC heating (top) and cooling (bottom) thermograms illustrating the thermotropic phase behavior of aqueous dispersions of DEPE in the absence of peptide. The thermograms that are shown were acquired at scan rates of 30 °C/h.

## RESULTS

DSC thermograms illustrating the thermotropic phase behavior of aqueous dispersions of DEPE are shown in Figure 1. In the heating mode, two fairly cooperative endothermic phase transitions occur. The more energetic phase transition centered near 37 °C corresponds to the L<sub>β</sub>–L<sub>α</sub> phase transition, and the less energetic phase transition centered near 65 °C corresponds to the L<sub>α</sub>–H<sub>II</sub> phase transition (see ref 3 and references therein). In the cooling mode, the H<sub>II</sub>–L<sub>α</sub> phase transition of DEPE exhibits considerable hysteresis, being centered near 58 °C, whereas the L<sub>α</sub>–L<sub>β</sub> phase transition exhibits less hysteresis but is split into two overlapping components. The splitting of the cooling exotherm of the L<sub>α</sub>–L<sub>β</sub> phase transition has also been observed with the linear saturated PEs (43, 44) and appears to be the result of domain inhomogeneities in the sample (44). Although we will briefly discuss the effects of incorporating the various transmembrane peptides studied on the L<sub>β</sub>–L<sub>α</sub> phase transition, the focus of this study is on the effects of these peptides on the L<sub>α</sub>–H<sub>II</sub> phase transition.

DSC heating thermograms illustrating the general effects of these transmembrane peptides on the L<sub>β</sub>–L<sub>α</sub> phase transition of aqueous dispersions of DEPE are shown in Figure 2. The thermograms were obtained from preparations composed of DEPE and the peptide L<sub>24</sub> and are typical of those exhibited by mixtures of DEPE with all of the peptides used in this study. It is clear that the incorporation of increasing quantities of L<sub>24</sub> progressively decreases the midpoint temperature and enthalpy and markedly increases the width (i.e., decreases the cooperativity) of the L<sub>β</sub>–L<sub>α</sub> phase transition of DEPE. Essentially identical effects on the L<sub>β</sub>–L<sub>α</sub> phase transition of DEPE were observed upon incorporation of peptides L<sub>24</sub>-DAP and W-L<sub>22</sub>-W (data not presented). These results are qualitatively similar to those observed upon incorporating comparable amounts of the closely related peptide P<sub>24</sub> into linear saturated PC and PE bilayers (16, 25) and thus confirm that the three peptides being studied here are being efficiently incorporated into the PE matrix.

DSC thermograms illustrating the general effects of these transmembrane peptides on the L<sub>α</sub>–H<sub>II</sub> phase transition of DEPE are shown in Figure 3. Again, the thermograms were obtained from preparations of DEPE and the peptide L<sub>24</sub> and are typical of those exhibited by mixtures of DEPE with L<sub>24</sub>-



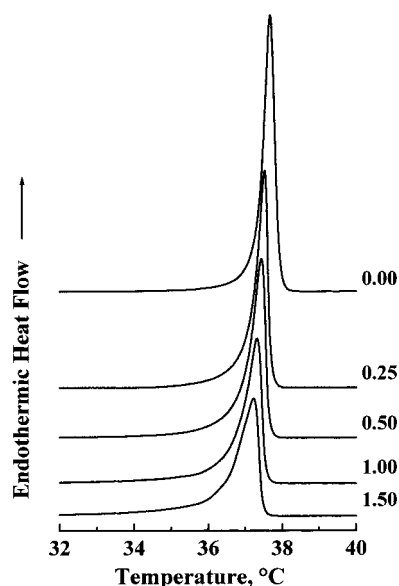


FIGURE 2: DSC heating thermograms illustrating the effect of incorporation of the peptide  $L_{24}$  on the  $L_{\beta}-L_{\alpha}$  phase transition of DEPE. The thermograms that are shown were acquired at the indicated peptide concentrations (mole percentage) and at a scan rate of 30 °C/h.

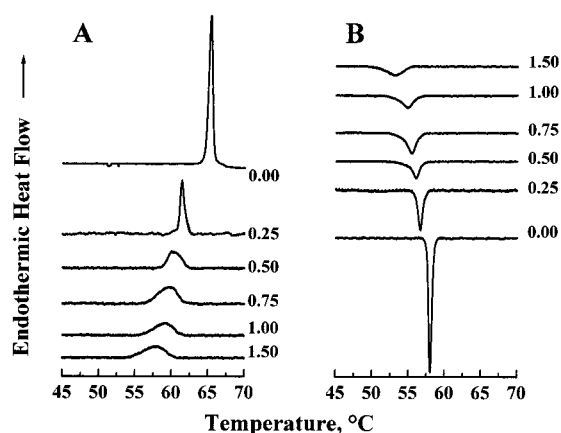


FIGURE 3: DSC heating (A) and cooling (B) thermograms illustrating the effect of the incorporation of peptide  $L_{24}$  on the  $L_{\alpha}-H_{II}$  phase transition of DEPE. The thermograms that are shown were acquired at scan rates of 30 °C/h and at the indicated peptide concentrations (mole percentage).

DAP and W- $L_{24}$ -W as well. It is clear that the incorporation of these peptides into DEPE vesicles results in a progressive decrease in the  $T_h$  as well as a marked decrease in the enthalpy (see Figure 4) and in the cooperativity of the  $L_{\alpha}-H_{II}$  phase transition. The effects of these peptides on the  $T_h$  of DEPE directly reflect their effects on the lamellar/nonlamellar phase-forming propensity of their lipid hosts and are the primary focus of this study.

The effect of variations in peptide concentration on the  $T_h$  of the DEPE matrix is presented in Figure 5. With the peptides  $L_{24}$ ,  $L_{24}$ -DAP, and W- $L_{22}$ -W, the  $T_h$  observed upon heating decreases fairly sharply at low ( $\leq 0.25$  mol %) levels of peptide incorporation, and less sharply at the higher peptide concentrations that were studied (0.25–1.5 mol %), where the decreases in  $T_h$  are a nearly linear function of peptide content. In the cooling mode, the initial decreases in  $T_h$  observed at low peptide concentrations are smaller than observed upon heating, but the incremental decreases in  $T_h$

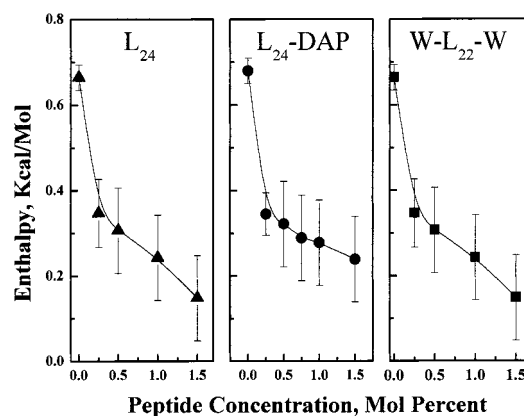


FIGURE 4: Effect of peptide concentration on the enthalpy of the  $L_{\alpha}-H_{II}$  phase transition of DEPE. The enthalpy values that are shown were derived from DSC heating thermograms obtained using a scan rate of 30 °C/h. The enthalpy values that are shown are the average and standard error from three determinations each on two independently prepared samples. The symbols used for mixtures of DEPE with each peptide are  $L_{24}$  ( $\blacktriangle$ ),  $L_{24}$ -DAP ( $\bullet$ ), and W- $L_{24}$ -W ( $\blacksquare$ ).

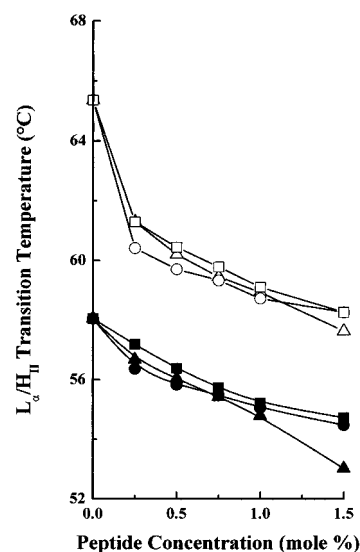


FIGURE 5: Effects of peptide concentration on the  $L_{\alpha}-H_{II}$  phase transition temperature of DEPE. The data were obtained from heating (white symbols) and cooling (black symbols) thermograms acquired at scan rates near 30 °C/h. The symbols used for mixtures of DEPE with each peptide are  $L_{24}$  ( $\blacktriangle$  or  $\triangle$ ),  $L_{24}$ -DAP ( $\bullet$  or  $\circ$ ), and W- $L_{22}$ -W ( $\blacksquare$  or  $\square$ ).

observed at higher peptide concentrations are comparable to those observed upon heating. Consequently, the overall decreases in  $T_h$  observed upon cooling are smaller than those observed in the corresponding heating experiment. It is thus clear that these transmembrane peptides all destabilize the  $L_{\alpha}$  phase of DEPE relative to its  $H_{II}$  phase, thus promoting the formation of the inverted nonlamellar phase at lower temperatures. It is also apparent that in both heating or cooling mode experiments, these three transmembrane peptides all induce comparable decreases in the  $T_h$  of the host lipid throughout the entire range of peptide concentrations that were examined. Thus, the characteristic effects of this class of  $\alpha$ -helical transmembrane peptides on both the lamellar gel–liquid-crystalline and liquid-crystalline lamellar–nonlamellar phase transitions of DEPE dispersions are general and are not significantly affected by the structural variations of the  $L_{24}$  peptide examined here.

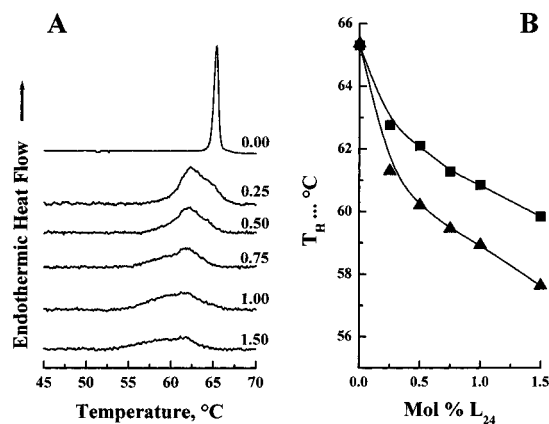


FIGURE 6: Effect of the incorporation of peptide P<sub>16</sub> on the L<sub>α</sub>–H<sub>II</sub> phase transition of DEPE. Panel A shows DSC heating thermograms of the L<sub>α</sub>–H<sub>II</sub> phase transitions exhibited by vesicles composed of DEPE and the peptide P<sub>16</sub>. The thermograms that are shown were acquired at scan rates of 30 °C/h at the indicated peptide concentrations (mole percentage). Panel B shows a comparison of the concentration-dependent changes in the  $T_h$  of DEPE induced by the peptides P<sub>16</sub> (■) and L<sub>24</sub> (▲).

Previous studies have demonstrated that a significant peptide-induced enhancement in membrane nonlamellar phase-forming propensity occurs when the lipid hydrophobic thickness significantly exceeds the hydrophobic length of the embedded transmembrane peptides (35, 36, 39, 40, 45–48). The effects of varying peptide length and lipid bilayer thickness on the lamellar/nonlamellar phase behavior of peptide-containing PE vesicles were thus examined to determine whether comparable hydrophobic mismatch effects are involved in the phenomena reported here. One series of measurements involved an examination of the effect of the peptide P<sub>16</sub> on the L<sub>α</sub>–H<sub>II</sub> phase transition of DEPE. The mean hydrophobic length of P<sub>16</sub>, expressed as the length of the polyleucine sequence measured at any point along the helix surface (see ref 17), is about 20–21 Å, approximately  $2/3$  of that of the peptides L<sub>24</sub>, W-L<sub>22</sub>-W, and L<sub>24</sub>-DAP (30–31 Å), and the hydrophobic length of P<sub>16</sub> should therefore be much shorter than the expected hydrophobic thickness of liquid-crystalline DEPE bilayers (~29 Å; see ref 49). DSC thermograms illustrating the effect of the peptide P<sub>16</sub> on the L<sub>α</sub>–H<sub>II</sub> phase transition of DEPE are shown in Figure 6 (left panel). As observed with the other peptides studied here, the incorporation of increasing quantities of P<sub>16</sub> into DEPE results in considerable broadening of the L<sub>α</sub>–H<sub>II</sub> phase transition endotherm. Moreover,  $T_h$  generally decreases as the peptide concentration increases, and as observed with the other peptides, this decrease is more pronounced at low peptide concentrations. However, the reductions of  $T_h$  observed with the P<sub>16</sub>/DEPE mixtures are significantly smaller than those of DEPE mixtures containing the longer peptides. This latter observation indicates that despite being significantly shorter than its host DEPE membrane host, the peptide P<sub>16</sub> is not as efficient at inducing nonlamellar phase formation in its host lipid membrane as are the longer peptides used in this study.

The second series of measurements involved an examination of the effect of the peptides L<sub>24</sub>, W-L<sub>22</sub>-W, and L<sub>24</sub>-DAP on the L<sub>α</sub>–H<sub>II</sub> transition of DPEPE, a shorter chain homologue of DEPE. In these experiments, the peptide hydrophobic length (30–31 Å) will more greatly exceed the lipid hydrophobic thickness (~25 Å; see ref 49) when

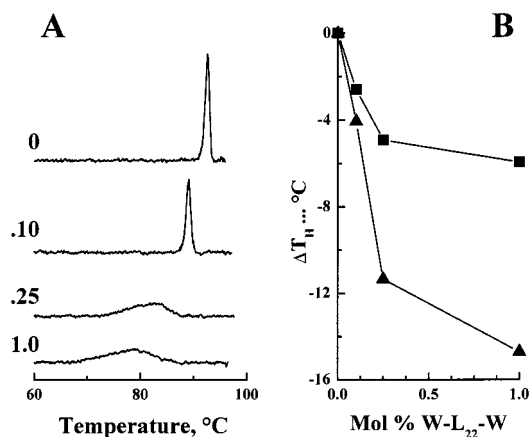


FIGURE 7: Effects of peptide incorporation on the L<sub>α</sub>–H<sub>II</sub> phase transition of DPEPE. Panel A shows DSC heating thermograms of the L<sub>α</sub>–H<sub>II</sub> phase transitions exhibited by vesicles composed of DPEPE and the peptide W-L<sub>22</sub>-W. The thermograms that are shown were acquired at scan rates of 30 °C/h at the indicated peptide concentrations (mole percentage). Panel B shows a comparison of the peptide-induced depression in the  $T_h$  of DPEPE (▲) and DEPE (■).

compared with the corresponding experiments using DEPE so that effects arising from this type of hydrophobic mismatch should be exaggerated. DSC thermograms which illustrate the effect of the peptides L<sub>24</sub>, W-L<sub>22</sub>-W, and L<sub>24</sub>-DAP on the L<sub>α</sub>–H<sub>II</sub> phase transition of DPEPE are shown in the left panel of Figure 7. DPEPE exhibits its L<sub>β</sub>–L<sub>α</sub> phase transition at temperatures near 20 °C and its L<sub>α</sub>–H<sub>II</sub> phase transition at temperatures near 92 °C (50). The incorporation of these peptides into DPEPE vesicles also causes a marked lowering of the  $T_h$  of the DPEPE lipid matrix as well as a decrease in the enthalpy and the cooperativity of the lipid L<sub>α</sub>–H<sub>II</sub> phase transition, results qualitatively similar to those observed with the corresponding DEPE/peptide mixtures. Also, the peptide concentration dependence of the peptide-induced decreases in the  $T_h$  of DPEPE is phenomenologically similar to that exhibited by the corresponding DEPE/peptide mixtures (Figure 7, left panel), although the magnitude of the decrease in  $T_h$  is considerably greater with the DPEPE/peptide mixtures. We also note that peptide-induced decreases in the L<sub>β</sub>–L<sub>α</sub> phase transition temperatures were also observed with the DPEPE/peptide mixtures examined here. However, unlike with the L<sub>α</sub>–H<sub>II</sub> phase transition, the magnitudes of the changes observed were comparable to those observed with the corresponding DEPE/peptide mixtures (data not shown).

Additional calorimetric experiments were performed to evaluate the possible influence of kinetic artifacts on the observations reported above. This possibility was suggested by the substantial cooling hysteresis which occurs at the H<sub>II</sub>–L<sub>α</sub> phase transition of DEPE (see Figure 1) and by previous indications that the kinetics of L<sub>α</sub>–H<sub>II</sub> phase transitions can be relatively slow because of the requirement for an interconversion between a two-dimensional and a three-dimensional lipid phase (51). These issues are particularly relevant to this work because the detection and accurate measurement of the thermodynamic properties of broad, weakly energetic phase transitions, such as the L<sub>α</sub>–H<sub>II</sub> phase transitions exhibited by many of the peptide-containing PE preparations that were examined, require relatively rapid heating or cooling of the sample. Thus, to determine whether

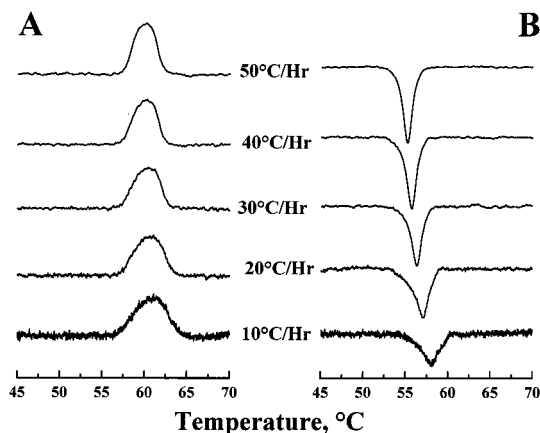


FIGURE 8: DSC heating (A) and cooling (B) thermograms illustrating the effect of scan rate on the  $L_\alpha$ – $H_{II}$  phase transitions that were examined. The thermograms that are shown were acquired at the indicated scan rates using DEPE samples containing 0.5 mol % peptide  $L_{24}$ . The areas under the DSC thermograms have been normalized to reflect variations in the scan rate that was utilized.

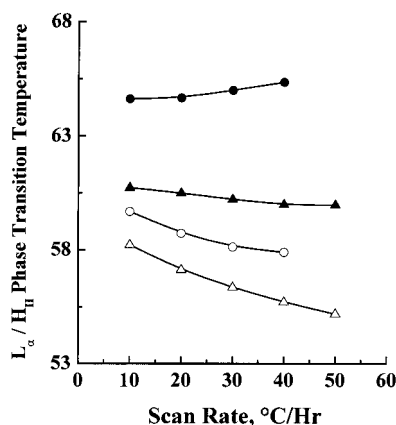


FIGURE 9: Effect of scan rate on the  $L_\alpha$ – $H_{II}$  phase transition temperatures of peptide-free (● and ○) and peptide-containing (▲ and △) DEPE vesicles. The data were acquired from both heating (black symbols) and cooling (white symbols) experiments. The peptide-containing DEPE sample contained 0.5 mol %  $L_{24}$ .

our results may have been affected by any differential effect of the incorporated transmembrane peptide on the kinetics, and thus the apparent temperature, of the  $L_\alpha$ – $H_{II}$  phase transition as measured by DSC, we carried out a series of experiments in which the scan rate dependencies of the  $T_h$  of peptide-free and peptide-containing DEPE samples were compared, and the results of such an experiment are shown in Figure 8. A comparison of the scan rate dependencies of the calorimetrically determined  $T_h$  values of peptide-free and peptide-containing DEPE vesicles is presented in Figure 9. With pure DEPE vesicles, increases in the heating scan rate ranging from 10 to 50 °C/h produce a relatively small increase ( $\sim 1$  °C) in the calorimetrically determined  $T_h$  values. Slightly larger decreases in  $T_h$  ( $\sim 2$  °C) are observed when the scan rate was varied in the cooling mode (see Figure 9). With the lipid/peptide mixtures, the same increases in heating scan rate result in a relatively small decrease ( $\sim 0.5$  °C) in the apparent  $T_h$  of the lipid/peptide mixture, and somewhat larger decreases in the apparent  $T_h$  in the corresponding cooling experiments (Figure 9). These results do indicate that there is a small kinetic component to calorimetrically determined  $T_h$  values recorded for DEPE and its mixtures with the transmembrane peptides. However, the magnitude

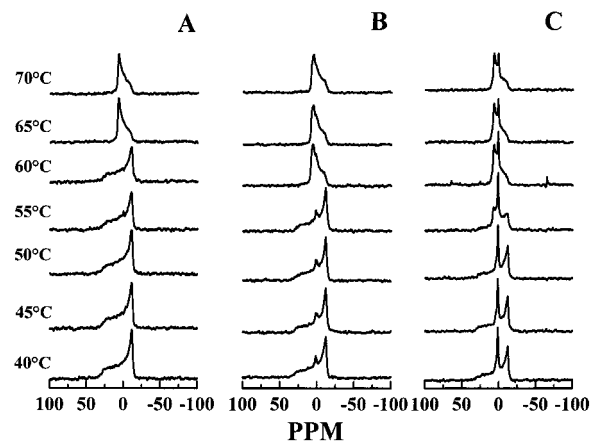


FIGURE 10: Proton-decoupled  $^{31}\text{P}$  NMR spectra exhibited by peptide-free (A) and peptide-containing (B and C) DEPE preparations. Sample B contained 0.5 mol %  $L_{24}$ , and sample C contained 1.5 mol %  $L_{24}$ . The spectra that are shown were acquired in the heating mode at the indicated temperatures.

of this effect is similar for peptide-free and peptide-containing DEPE dispersions and is clearly smaller than the observed peptide-induced changes in  $T_h$ . We therefore conclude that the observed peptide-induced decreases in  $T_h$  are the result of real shifts in the  $L_\alpha$ – $H_{II}$  phase equilibrium and not the result of kinetic artifacts.

$^{31}\text{P}$  NMR spectroscopic measurements were also performed to determine the nature of the various lamellar–nonlamellar phase transitions exhibited by the peptide-containing vesicles examined in this study. As illustrated in Figure 10A, aqueous dispersions of DEPE exhibit so-called axially symmetric  $^{31}\text{P}$  NMR powder patterns at temperatures below the onset of the  $L_\alpha$ – $H_{II}$  phase transition of the lipid. Such powder patterns are typical of those exhibited by phospholipid bilayers in which the phosphate headgroup reorientational motions are fast and axially symmetric on the  $^{31}\text{P}$  NMR time scale (52). At temperatures above the calorimetrically determined  $L_\alpha$ – $H_{II}$  phase transition, the powder pattern narrows significantly and its shape changes abruptly to one characteristic of phospholipid headgroups undergoing fast orientational motions in an inverted hexagonal assembly (53). As expected, these results are consistent with the conversion of an  $L_\alpha$  phase to an  $H_{II}$  phase at temperatures coinciding with the calorimetrically observed heating endotherm near 65 °C. Figure 10 also shows that the DEPE/peptide mixtures that were examined begin to exhibit  $^{31}\text{P}$  NMR signatures of  $H_{II}$  phases at lower temperatures than with pure DEPE dispersions, in a peptide concentration-dependent manner. Thus, with mixtures containing 0.5 mol % peptide,  $^{31}\text{P}$  NMR signatures consistent with the retention of lamellar structures are observed at temperatures near 55 °C and powder patterns consistent with complete conversion to the  $H_{II}$  phase are observed at temperatures near 60 °C (Figure 10B). At peptide concentrations near 1.5 mol %, our  $^{31}\text{P}$  NMR spectroscopic data also show that the onset of  $H_{II}$  phase formation occurs at temperatures near 55 °C and is substantially complete at temperatures near 60 °C (Figure 10C), observations in excellent agreement with the results of our DSC experiments. However, the data also show that the  $^{31}\text{P}$  NMR spectra of the peptide-containing samples also contain nontrivial contributions from a resonance peak at the so-called isotropic

frequency (Figure 10B,C) and that the relative intensity of this peak increases with increasing peptide concentration. The structural basis of the appearance of this signal is unclear at this time but could, in principle, be an indication of the presence of small fast tumbling vesicular structures or three-dimensionally ordered lipid structures such as inverted cubic phases (53), most likely the latter. Nevertheless, it is clear that such structures form only a small fraction of the overall phospholipid population throughout most of the range of peptide concentrations that were examined and that the dominant structural change being monitored in our calorimetric experiments is in fact the  $L_{\alpha}$ - $H_{II}$  phase transition of the PE matrix, even at the highest peptide concentrations that were tested.

## DISCUSSION

The most important finding of this study is that small amounts of the three  $\alpha$ -helical transmembrane peptides ( $L_{24}$ , W- $L_{22}$ -W, and  $L_{24}$ -DAP) significantly lower the  $L_{\alpha}$ - $H_{II}$  phase transition temperature of the PE matrixes into which they insert and that this effect is qualitatively and quantitatively comparable when each of these three peptides is incorporated into the same PE matrix. Peptide-induced promotion of lipid nonlamellar phase formation has been the subject of many theoretical considerations (see refs 35, 36, 54, and 55 and references therein) and has been observed experimentally in lipid bilayers containing the amphipathic  $\alpha$ -helical peptide alamethicin (28), the channel-forming antimicrobial peptide gramicidin A (refs 15, 35, 36, and 48 and references therein), and the cyclic  $\beta$ -sheet-forming antimicrobial peptide gramicidin S (29), and has recently been observed in lipid bilayers containing a number of synthetic tryptophan-anchored transmembrane peptides, the "WALP" peptides (45–47). However, the mechanism(s) whereby such peptides induce or otherwise potentiate the formation of nonlamellar phases in their host lipid matrixes is currently unknown, and it is not clear whether our experimental observations are mechanistically comparable to any of the previously reported instances of peptide-induced enhancement of lipid nonlamellar phase formation. The mechanistic basis for the peptide-induced enhancement of lipid nonlamellar phase-forming propensity is an unresolved issue which is under active investigation in many laboratories.

It is interesting to compare the general findings of these studies with the spectroscopic and X-ray diffraction studies of Killian and co-workers, who examined the effects of various ditryptophan-anchored (40, 45–47) and dilysine-anchored (39) transmembrane peptides on the lamellar/nonlamellar phase behavior of phospholipid bilayers. These authors demonstrated that the tryptophan-anchored (WALP) peptides markedly enhance the nonlamellar phase-forming propensities of their host membranes under conditions where the lipid bilayer hydrophobic thickness significantly exceeds the hydrophobic length of the peptide (40, 45–47), observations similar to those reported in comparable studies of the interaction of gramicidin A with phospholipid bilayers (15, 35, 36, 48). They also demonstrated that the peptides WALP-27 and WALP-31 were considerably less efficient at promoting nonlamellar phase formation in DEPE and DOPE/DOPG membranes (40, 47), presumably because their hydrophobic lengths more closely match the hydrophobic thickness of the

lipid matrix. There were also indications that WALP-31 (the longest of the WALP peptides used) may not be completely miscible with the  $L_{\alpha}$  and  $H_{II}$  phases of dielaidoyl or dioleoyl phospholipids, presumably because its hydrophobic length greatly exceeds the probable hydrophobic thickness of these lipids, especially at temperatures above the  $T_h$  (40, 47). In these respects, the behavior of the WALP peptides contrasts sharply with that of our dilysine-anchored peptides, which cause a significant enhancement of the nonlamellar phase-forming propensities of their host PE membranes under conditions where peptide hydrophobic length is either comparable to or significantly greater than the expected hydrophobic thickness of the liquid-crystalline lipid membrane hosts. Interestingly, Killian and co-workers also demonstrated that some dilysine-anchored model transmembrane peptides (KALPs) can also induce the formation of nonlamellar phases under conditions where membrane hydrophobic thickness greatly exceeds peptide hydrophobic length (39). However, the KALP peptides were shown to be less potent inducers of nonlamellar phase formation than the corresponding WALP analogues, and evidence of nonlamellar phase formation was only obtained when the KALP peptides were incorporated into membranes composed of unsaturated phospholipids with very long chains. The authors therefore concluded that the induction of nonlamellar phases by the WALP and KALP series of peptides was driven by the hydrophobic mismatch stress which occurs when membrane hydrophobic thickness significantly exceeds peptide hydrophobic length, and the difference between the nonlamellar phase-inducing properties of comparable WALP and KALP peptides was ascribed to differences in the affinities of the anchoring tryptophan and lysine residues for the polar–apolar interfacial regions of their membrane hosts (39). In these studies, we also demonstrate that dilysine-anchored transmembrane peptides can enhance the nonlamellar phase-forming propensity of their PE membrane hosts. However, as shown below, our data cannot be rationalized within the framework of the hydrophobic mismatch effects described by Killian and co-workers.

We have clearly demonstrated here that our dilysine-anchored peptides ( $L_{24}$ , W- $L_{22}$ -W, and  $L_{24}$ -DAP) significantly enhance the lamellar/nonlamellar phase-forming propensity of DEPE model membranes under conditions where peptide hydrophobic length exceeds membrane hydrophobic thickness. Moreover, the magnitude of this effect increases when these same peptides are incorporated into a thinner membrane (see Figure 7, right panel) and decreases when a shorter peptide is incorporated into the DEPE matrix (see Figure 6, right panel). These observations are the opposite of the hydrophobic mismatch effects reported by Killian and co-workers. The basis of these phenomenological differences between our results and those obtained in studies of gramicidin A and of the WALP and KALP series of peptides is not clear. However, some of these differences could arise, in part, from the different methodologies employed in the different laboratories. For example, the decreases in the  $T_h$  of DEPE observed in our DSC experiments ( $\sim 6$ – $8$  °C at peptide concentrations near 1.5 mol %) are smaller than the temperature resolution of the comparable  $^{31}\text{P}$  NMR spectroscopic studies performed by Killian and co-workers ( $\sim 10$  °C; see ref 40), and it is therefore possible that the peptides WALP-27 and WALP-31 could have had effects comparable



to those observed by us that were not detected in these earlier studies. Whether these differences are the cause of, or significant contributors to, the phenomenological differences noted above remains to be determined.

Our studies also show that the extent of destabilization of the L<sub>α</sub> phase relative to the H<sub>II</sub> phase of DEPE is not affected by the replacement of each of the leucine residues at the ends of the hydrophobic core of L<sub>24</sub> with tryptophan residues, or by replacing each of the two positively charged lysine residues at the two ends of L<sub>24</sub> with the shorter side chain but still positively charged amino acid analogue DAP. Thus, the alteration of the lamellar-inverted nonlamellar phase equilibrium of the DEPE matrix stems from the general overall structure of these peptides and is apparently insensitive to the modifications tested here. However, with peptides such as gramicidin A, seemingly small modifications of the chemical structure of the peptide (e.g., formylation of the terminal tryptophans) completely abolishes the capacity to induce formation of lipid nonlamellar phases (37, 38). Also, Killian and co-workers have shown that a change in the nature of the amino acid residues anchoring an alternating stretch of leucine and alanine residues (note the differences between the WALP and KALP series of peptides) can also markedly alter their capacity to induce nonlamellar phases in their membrane hosts (39). An obvious difference between our work and those involving gramicidin A and the WALP and KALP series of peptides is the fact that the polyleucine cores of the helical peptides used here are intrinsically more hydrophobic and more conformationally stable than the poly-(Leu-Ala) cores of the WALP and KALP series of peptides (see ref 41). It is therefore possible that the greater hydrophobicity and conformational stability which the polyleucine core confers upon our peptides may make their nonlamellar phase-inducing properties less sensitive to the "end-group" modifications employed in these studies.

A common feature of our results and some of the data presented elsewhere (47) is the fact that the incorporation of relatively small amounts of transmembrane peptide can induce seemingly disproportionately large decreases in the *T<sub>h</sub>* of the host membrane. We have shown in this study that the enthalpy of the L<sub>α</sub>-H<sub>II</sub> phase transition is also markedly and disproportionately reduced at very low peptide concentrations. Recently, Morein et al. (47) suggested that peptide concentrations near 0.25 mol % are probably insufficient to globally alter the spontaneous curvature or packing properties of the lipid membrane to an extent consistent with the magnitude of the observed depression in *T<sub>h</sub>*, and that the mechanistic basis of the changes in nonlamellar phase behavior observed at low peptide concentrations may not be the same as that operating at higher concentrations. Our <sup>31</sup>P NMR spectroscopic studies also show that concomitant with the peptide-induced lowering of the L<sub>α</sub>-H<sub>II</sub> phase transition temperature, there was a small coexisting phospholipid population undergoing fast isotropic motion on the <sup>31</sup>P NMR time scale (possibly a cubic phase) and that the size of this population increases with increases in peptide concentration. The possibility that our lipid/peptide preparations may preferentially form cubic phases instead of H<sub>II</sub> phases at higher peptide concentrations is consistent with the suggestions of Morein et al. (47).

Finally, we note that our experimental results provide neither positive nor negative evidence for the so-called

"snorkel effect" of the terminal lysine residues in modulating the effects a hydrophobic mismatch between peptide hydrophobic length and membrane hydrophobic thickness, mainly because the effects of our peptides on the lamellar/nonlamellar phase behavior of their host membrane do not appear to be primarily governed by hydrophobic mismatch effects in any case. Consequently, these experiments do not provide a crucial test of whether the flexible side chains of lysine residues near the ends of transmembrane peptide helices can alter the effective hydrophobic lengths of such peptides.

## ACKNOWLEDGMENT

We are indebted to Dr. Brian D. Sykes of the Department of Biochemistry at the University of Alberta for the generous availability of time on the NMR spectrometer.

## REFERENCES

- Gennis, R. B. (1989) *Biomembranes. Molecular Structure and Function*, Springer-Verlag, New York.
- Yeagle, P. (1992) *The Structure of Biological Membranes*, CRC Press, Boca Raton, FL.
- Lewis, R. N. A. H., Mannock, D. A., and McElhaney, R. N. (1997) in *Current Topics in Membranes* (Epand, R. M., Ed.) Vol. 44, pp 25–102, Academic Press, New York.
- Rilfors, L., Lindblom, G., Wieslander, A., and Christiansson, A. (1984) in *Membrane Fluidity* (Kates, M., and Manson, L. A., Eds.) pp 205–245, Plenum Press, New York.
- Thurmond, R. L., and Lindblom, G. (1997) in *Lipid Polymorphism and Membrane Properties* (Epand, R. M., Ed.) pp 103–166, Academic Press, San Diego.
- Lewis, R. N. A. H., and McElhaney, R. N. (1995) *Biochemistry* 34, 13818–13824.
- Foht, P. J., Tran, Q. M., Lewis, R. N. A. H., and McElhaney, R. N. (1995) *Biochemistry* 34, 13811–13817.
- Hui, S. W. (1997) in *Lipid Polymorphism and Membrane Properties* (Epand, R. M., Ed.) pp 541–563, Academic Press, San Diego.
- Israelachvili, J. (1992) *Intermolecular and Surface Forces*, pp 366–394, Academic Press, San Diego.
- Cevc, G., and Marsh, D. (1987) *Phospholipid Bilayers. Physical Principles and Models*, pp 407–425, John Wiley and Sons, New York.
- Lee, Y. C., Zheng, Y. O., Taraschi, T. F., and Janes, N. (1996) *Biochemistry* 35, 3677–3684.
- Lee, Y.-C., Taraschi, T. F., and James, N. (1993) *Biophys. J.* 65, 1429–1432.
- Janes, N. (1996) *Chem. Phys. Lipids* 81, 133–150.
- Epand, R. M. (1997) in *Current Topics in Membranes* (Epand, R. M., Ed.) Vol. 44, pp 237–252, Academic Press, New York.
- Davis, J. H., Clare, D. M., Hodges, R. S., and Bloom, M. (1983) *Biochemistry* 22, 5298–5305.
- Killian, J. A. (1998) *Biochim. Biophys. Acta* 1376, 401–416.
- Zhang, Y.-P., Lewis, R. N. A. H., Hodges, R. S., and McElhaney, R. N. (1992) *Biochemistry* 31, 11579–11588.
- Zhang, Y.-P., Lewis, R. N. A. H., Hodges, R. S., and McElhaney, R. N. (1992) *Biochemistry* 31, 11572–11578.
- Axelsen, P. H., Kaufman, B. K., McElhaney, R. N., and Lewis, R. N. A. H. (1995) *Biophys. J.* 69, 2770–2781.
- Huschilt, J. C., Millman, B. M., and Davis, J. H. (1989) *Biochim. Biophys. Acta* 979, 139–141.
- Bolen, E. J., and Holloway, P. W. (1990) *Biochemistry* 29, 9638–9643.
- Huschilt, J. C., Hodges, R. S., and Davis, J. H. (1985) *Biochemistry* 24, 1377–1386.
- Morrow, M. R., Huschilt, J. C., and Davis, J. H. (1985) *Biochemistry* 24, 5396–5406.
- Zhang, Y.-P., Lewis, R. N. A. H., Hodges, R. S., and McElhaney, R. N. (1995) *Biophys. J.* 68, 847–857.

25. Pauls, K. P., MacKay, A. L., Soderman, O., Bloom, M., Taneja, A. K., and Hodges, R. S. (1985) *Eur. Biophys. J.* 12, 1–11.
26. Subczynski, W. K., Lewis, R. N. A. H., McElhaney, R. N., Hodges, R. S., Hyde, J. S., and Kusumi, A. (1998) *Biochemistry* 37, 3156–3164.
27. Keller, S. L., Gruner, S. M., and Gawrisch, K. (1996) *Biochim. Biophys. Acta* 1127, 241–246.
28. Prenner, E. J., Lewis, R. N. A. H., Neuman, K. C., Gruner, S. M., Kondejewski, L. H., Hodges, R. S., and McElhaney, R. N. (1997) *Biochemistry* 36, 7906–7916.
29. van Echtheld, C. J. A., van Strigt, R., de Kruijff, B., Leunissen-Bijvelt, J., Verkleij, A. J., and De Geir, J. (1981) *Biochim. Biophys. Acta* 648, 287–291.
30. Killian, J. A., and de Kruijff, B. (1985) *Biochemistry* 24, 7881–7890.
31. van der Wel, P. C. A., Pott, T., Morein, S., Greathouse, D. V., Koeppe, R. E., and Killian, J. A. (2000) *Biochemistry* 39, 3124–3133.
32. Segrest, J. P., De Loof, H., Dohlman, J. G., Brouillette, C. G., and Anantharamaiah, G. M. (1990) *Proteins: Struct., Funct., Genet.* 8, 103–117.
33. Monne, M., Nilsson, I., Johansson, M., Elmhed, N., and von Heijne, G. (1998) *J. Mol. Biol.* 284, 1177–1183.
34. Preusch, P. C., Norvell, J. C., Cassatt, J. C., and Cassman, M. (1998) *Nat. Struct. Biol.* 5, 12–14.
35. Killian, J. A., and de Kruijff, B. (1988) *Biophys. J.* 53, 111–117.
36. Killian, J. A. (1992) *Biochim. Biophys. Acta* 1113, 391–425.
37. Killian, J. A., Timmermans, J. W., Keur, S., and de Kruijff, B. (1985) *Biochim. Biophys. Acta* 820, 154–156.
38. Aranda, F. J., Killian, J. A., and de Kruijff, B. (1987) *Biochim. Biophys. Acta* 901, 217–228.
39. de Planque, M. R. R., Keuijtz, J. A. W., Liskamp, R. M. J., Marsh, D., Greathouse, D. V., Koeppe, R. E., de Kruijff, B., and Killian, J. A. (1999) *J. Biol. Chem.* 274, 20839–20846.
40. Van der Wel, P. C. A., Pott, T., Morein, S., Greathouse, D. V., Koeppe, R. E., and Killian, J. A. (2000) *Biochemistry* 39, 3124–3133.
41. Zhang, Y.-P., Lewis, R. N. A. H., Henry, G. D., Sykes, B. D., Hodges, R. S., and McElhaney, R. N. (1995) *Biochemistry* 34, 2348–2361.
42. Lewis, R. N. A. H., Sykes, B. D., and McElhaney, R. N. (1988) *Biochemistry* 27, 880–887.
43. Lewis, R. N. A. H., and McElhaney, R. N. (1993) *Biophys. J.* 64, 1081–1096.
44. Yao, H., Hatta, I., Koynova, R., and Tenchov, B. (1992) *Biophys. J.* 61, 683–693.
45. Killian, J. A., Salemink, I., De Planque, M. R. R., Lindblom, G., Koeppe, R. E., and Greathouse, D. V. (1996) *Biochemistry* 35, 1037–1045.
46. Morein, S., Strandberg, E., Killian, J. A., Persson, S., Arvidson, G., Koeppe, R. E., and Lindblom, G. (1997) *Biophys. J.* 73, 3078–3088.
47. Morein, S., Koeppe, R. E., Lindblom, G., de Kruijff, B., and Killian, J. A. (2000) *Biophys. J.* 78, 2475–2485.
48. Watnick, P. I., Dea, P., and Chan, S. I. (1990) *Biochemistry* 29, 6215–6221.
49. Harper, P. E., Lewis, R. N. A. H., Mannock, D. A., McElhaney, R. N., and Gruner, S. M. (2001) *Biophys. J.* (in press).
50. Silvius, J. R., Lyons, M., Yeagle, P. L., and O’Leary, T. J. (1985) *Biochemistry* 24, 5388–5395.
51. Caffrey, M. (1985) *Biochemistry* 24, 4826–4844.
52. Seelig, J. (1978) *Biochim. Biophys. Acta* 515, 105–140.
53. Tilcock, C. P. S., Cullis, P. R., and Gruner, S. M. (1986) *Chem. Phys. Lipids* 40, 47–56.
54. Cornell, B. A., and Separovic, F. (1988) *Eur. Biophys. J.* 16, 299–306.
55. May, S., and Ben-Shaul, A. (1999) *Biophys. J.* 76, 751–767.

BI001942J